

# Size Characterization of Incinerator Fly Ash Using Sedimentation/Steric Field-Flow Fractionation

Won-Suk Kim<sup>†</sup> and Dai Woon Lee<sup>\*</sup>

Department of Chemistry, Yonsei University, Seoul 120-749, Korea

Seungho Lee

Department of Chemistry, Hannam University, Taejon 306-791, Korea

**Fly ash particles emitted from municipal solid waste-incinerators are of environmental concern. This study aims to investigate the applicability of sedimentation/steric field-flow fractionation (Sd/StFFF) and to develop a Sd/StFFF method for the separation and size characterization of incinerator fly ash. This study focuses on the fly ash particles larger than  $\sim 1\ \mu\text{m}$ , which comprise more than 90% (w/w) of the fly ash. Fly ash is a complex mixture of particles having various chemical compositions, sizes, shapes, and densities. Prior to Sd/StFFF analysis, fly ash particles are prefractionated into six density classes using a modified centrifugal procedure. It was found that fly ash particles are most abundant in the density range between 2.4 and 2.8 g/cm<sup>3</sup>. Different density fractions seem to contain particles of different chemical compositions. The Sd/StFFF conditions for the size-characterization of fly ash are sample concentration,  $\sim 0.3\%$  (w/v); dispersing medium, 50% ethanol in water; and carrier liquid, water with 1.0% FL-70 (ionic strength  $\sim 0.012\ \text{M}$ ). Sd/StFFF data show no significant differences in size distribution among different density fractions. Generally, the sizes obtained from Sd/StFFF are larger than those obtained from a Coulter Multisizer and microscopy, probably because of the irregular shapes of the fly ash particles.**

Interest in nanometer- to micrometer-sized particulate materials is growing in environmental and high technology industries,<sup>1–3</sup> because those particulates play important roles in the transfer of various toxic compounds (pollutants) exposed to air, water, and soil.<sup>4,5</sup> Various chemical and physical properties (such as size or morphology) of environmental particles directly affect the transfer

mechanism of toxic compounds in environmental systems<sup>6</sup> and, thus, need to be accurately determined to understand the transfer mechanism.

Incinerator fly ash is generated from nonvolatile inorganics and unburned constituents of coal and waste during combustion. As the char fragments and burns out, these micrometer-sized molten droplets (mixtures of clay minerals composed primarily of alumina and silica, with small amounts of iron oxide, calcia, and others) are entrained, and swept out of the combustor with the flue gas.<sup>7,8</sup> Fly ash has an unusually broad size distribution, with diameters spanning more than 3 orders of magnitude,<sup>9–11</sup> and it is extremely complex in both physical and chemical properties, making the accurate analysis of incinerator fly ash difficult. In general, fly ash has a multimodal distribution.<sup>9,12</sup> It has been found that a large fraction of fly ash consists of particles having a size range of  $\sim 1\text{--}100\ \mu\text{m}$ , for which the concentration of trace elements is inversely related to the particle size. In the submicrometer size range, concentration is found to be independent of the particle size.<sup>10</sup> It would seem to indicate that there exists at least two different mechanisms of fly ash formation.

The size and size distribution of fly ash are important, because they influence the transport pathway of pollutants and the degree of penetration of the ash particles into the human respiratory system. The effect of particle size on the adsorption characteristics of toxic chemicals has been studied for coal fly ash, in which the formation mechanism and the relationship of the particle size with the amount of toxic inorganic species, such as heavy metals, have been investigated.<sup>9,13,14</sup> Still, the fly ash emitted from municipal solid-waste incinerators has not yet been studied much, because

<sup>\*</sup> Corresponding author. Phone: +82-2-2123-2635. Fax: +82-2-364-7050. E-mail: leedw@yonsei.ac.kr.

<sup>†</sup> Present address: Department of Chemistry, University of Illinois, Urbana, IL 61801.

(1) Donaldson, K.; Li, X. Y.; MacNee, W. J. *Aerosol. Sci.* **1998**, *29*, 553–560.

(2) Oberdorster, G. *Inhalation Toxicol.* **1996**, *8*, 73–90.

(3) Liu, J.; Rinzler, A. G.; Dai, H.; Hafner, J. H.; Bradley, R. K.; Boul, P. J.; Lu, A.; Iverson, T.; Shelimov, K.; Huffman, C. B.; Rodriguez-Macias, F.; Shon, Y. S.; Lee, T. R.; Cobert, D. T.; Smalley, R. E. *Science* **1998**, *280*, 1253–1256.

(4) Klein, T.; Niessner, R. *Mikrochim. Acta* **1998**, *129*, 47–55.

(5) Van Jaarsveld, J. A.; Schutter, M. A. A. *Chemosphere* **1993**, *27*, 131–139.

(6) Cuddihy, R. G.; Griffith, W. C.; McClellan, R. O. *Environ. Sci. Technol.* **1984**, *18*, 14A–21A.

(7) S. Ghosal, Ph.D. Thesis, Stanford University, Stanford, CA, 1993.

(8) Ibáñez, R.; Andrés, A.; Viguri, J. R.; Ortiz, I.; Irabien, J. A. *J. Hazard. Mater. A* **2000**, *79*, 215–227.

(9) Natusch, D. F. S.; Wallace, J. R.; Evans, C. A., Jr. *Science* **1974**, *183*, 202–204.

(10) Graff, K. A.; Caldwell, K. D.; Myers, M. N.; Giddings, J. C. *Fuel* **1984**, *63*, 621–626.

(11) Ghosal, S.; Self, S. A. *Fuel* **1995**, *74*, 522–529.

(12) Giddings, J. C.; Graff, K. A.; Myers, M. N.; Caldwell, K. D. *Sep. Sci. Technol.* **1980**, *15*, 615–635.

(13) Conzemius, R. J.; Welcomer, T. D.; Svec, H. J. *Environ. Sci. Technol.* **1984**, *18*, 12–18.

(14) Furuya, K.; Miyajima, Y.; Chiba, T.; Kikuchi, T. *Environ. Sci. Technol.* **1987**, *21*, 898–903.

of the complexity in its composition and physicochemical properties, such as density and size. Earlier studies on the analysis of incinerator fly ash have been primarily focused on the determination of the bulk chemical composition of the fly ash particles. The chemicals of primary interest have been polychlorinated biphenyls (PCBs), polychlorinated dibenzo-*p*-dioxins (PCDDs), polychlorinated dibenzofurans (PCDFs), polycyclic aromatic hydrocarbons (PAHs), and some inorganic compounds, such as heavy metals and metal complexes.<sup>15–17</sup> The relationship between the particle size and the chemical composition has not yet been investigated.

A number of methods have been employed for the sizing of fly ash particles emitted from power plants and municipal solid-waste incinerators, which include a cascade impactor,<sup>15</sup> a Coulter Multisizer,<sup>11</sup> and an electric low-pressure impactor.<sup>18</sup> Recently, with the advent of aerosol time-of-flight mass spectrometry (ATOFMS), it is now possible to measure the size and the mass spectrum of a single particle.<sup>19</sup> Each method has its own merits and shortcomings in particle sizing.

The cascade impactor yields the aerodynamic diameter,<sup>15,20</sup> which can be converted into a geometrical size if the density is known. Accurate sizing may not be possible for particle samples having broad density distributions. Similarly, standard sedimentation techniques (such as the Andreasen pipet method) yield size distributions based on the Stokes diameter (not on the geometrical diameter).<sup>21</sup> Static light scattering (SLS) provides size information in an absolute sense (without the need for calibration). The application of SLS may not be suitable for the sizing of particles having various chemical compositions, since the optical property varies with the chemical composition. The optical sizing has been performed by SLS using a geometric approximation.<sup>22</sup> Ultrasonic sieving has been used for the disaggregation and the fractionation of fly ash particles into a lot of size bins.<sup>14</sup> The application of the ultrasonic sieving is limited down to  $\sim 5 \mu\text{m}$  (no further fractionation for particles smaller than  $\sim 5 \mu\text{m}$ ). Microscopy has also been used to determine particle size distribution.<sup>23,24</sup> There are statistical artifacts associated with image analysis, because only a part of the population is analyzed.<sup>24</sup> In contrast to other techniques, the diameter measured by the Coulter Multisizer is independent of the density or the refractive index of the particle.<sup>7,11</sup> The diameter reported is actually the diameter of a sphere with the same volume as that of the particle. Although the Coulter Multisizer has a relatively broad dynamic range, it is still limited by the orifice size (usually between 2 and 60% of the diameter of the orifice). In

addition, the Coulter data tend to vary with the suspension concentration. In general, the Coulter Multisizer seems to be better suited than others for the sizing of complex powders, such as fly ash, whose density varies from particle to particle.

Field-flow fractionation (FFF) is a separation technique that is applicable to particulates and macromolecules.<sup>25,26</sup> It has been shown that FFF is potentially useful for size characterization of engine soot particles.<sup>27–29</sup> Being an elution technique, FFF also allows narrow fractions of particles to be collected and subjected to further analysis by other analysis tools. FFF has been used in combination with on- or off-line with microscopy,<sup>29,30</sup> inductively coupled plasma mass spectrometry (ICPMS),<sup>31,32</sup> energy-dispersive X-ray analyzer (EDX),<sup>33</sup> and light scattering.<sup>34,35</sup>

Among various FFF subtechniques, the steric mode of sedimentation FFF (Sd/StFFF) is particularly useful for the separation of particles larger than  $\sim 1 \mu\text{m}$  with high resolution and speed. For spherical particles of the constant density, Sd/StFFF FFF provides size-based separation, and thus, the Sd/StFFF elution profile ("fractogram") can be easily converted to the size distribution. The combination of high resolution and high speed with system flexibility has made Sd/StFFF an attractive tool for the analysis of various particulate materials, including biological cells,<sup>36</sup> chromatographic supports,<sup>37</sup> and industrial materials.<sup>38</sup> This study is aimed at investigating the applicability of Sd/StFFF and developing a Sd/StFFF method for the separation and size characterization of incinerator fly ash. This study is focused on the size analysis of those particles larger than  $\sim 1 \mu\text{m}$ , which constitutes more than 90% (w/w) of fly ash.

## EXPERIMENTAL SECTION

**Materials.** The particle standards used in this study are polystyrene-divinyl benzene copolymer latex beads (Duke Scientific Corporation, Palo Alto, CA) having nominal diameters (determined by transmission electron microscopy) of 40, 29.9, 20, 15, 9.87, 7, 5.01, 4, 3.004, and 2.013  $\mu\text{m}$  (hereafter referred to as 40, 30, 20, 15, 10, 7, 5, 4, 3, and 2  $\mu\text{m}$ , respectively). The particle standards were mixed without dilution for preparation of a standard mixture.

Fly ash sample was collected in a bag filter at the Changwon municipal incinerator in Korea. The fly ash particles were recovered from the bag filter, dispersed in water with 0.1% FL-70,

- (15) Kaupp, H.; Towara, J.; McLachlan, M. S. *Atmos. Environ.* **1994**, *28*, 585–593.
- (16) Kurokawa, Y.; Takahiko, M.; Matayoshi, N.; Satoshi, T.; Kazumi, F. *Chemosphere* **1998**, *37*, 2161–2171.
- (17) Pistikopoulos, P.; Wortham, H. M.; Gomes, L.; Masclet-Beyne, S.; Bon Nguyen, E.; Masclet, P. A.; Mouvier, G. *Atmos. Environ.* **1990**, *24A*, 2573–2584.
- (18) Pitts, J. H.; Finlayson-Pitts, B. J. *Atmospheric Chemistry: Fundamentals and Experimental Techniques*; John Wiley & Sons: New York, 1986.
- (19) Noble, C. A.; Prather, K. A. *Environ. Sci. Technol.* **1996**, *30*, 2667–2680.
- (20) Newton, G. J.; Raabe, O. G.; Mokler, B. V. *J. Aerosol. Sci.* **1977**, *8*, 339–347.
- (21) Allen, T. *Particle Size Measurement*; Chapman and Hall: London, 1981.
- (22) Diamond, S. *Mater. Res. Soc. Sym. Proc.* **1988**, *113*, 119–127.
- (23) Norton, G. A.; Markuszewski, R.; Shanks, H. R. *Environ. Sci. Technol.* **1986**, *20*, 409–413.
- (24) Rincon, J. M.; Romero, M.; Boccacini, A. R. *J. Mater. Sci.* **1999**, *34*, 4413–4423.

- (25) Giddings, J. C. *Science* **1993**, *260*, 1456–1465.
- (26) Giddings, J. C. *Anal. Chem.* **1995**, *67*, 592A–598A.
- (27) Kirkland, J. J.; Liebold, W.; Unger, K. K. *J. Chromatogr. Sci.* **1990**, *28*, 374–378.
- (28) Kim, W. S.; Park, Y. H.; Shin, J. Y.; Lee, D. W.; Lee, S. *Anal. Chem.* **1999**, *71*, 3265–3272.
- (29) Kim, W. S.; Kim, S. H.; Lee, S.; Lim, C. S.; Ryu, J. H. *Environ. Sci. Technol.* **2001**, *35*, 1005–1012.
- (30) Lee, S.; Rao, S. P.; Moon, M. H.; Giddings, J. C. *Anal. Chem.* **1996**, *68*, 1545–1549.
- (31) Taylor, H. E.; Garbarino, J. R.; Murphy, D. M.; Beckett, R. *Anal. Chem.* **1992**, *64*, 2035–2041.
- (32) Hassellöv, M.; Lyvén, B.; Haraldsson, C.; Sirinawin, W. *Anal. Chem.* **1999**, *71*, 3497–3502.
- (33) Karaiskakis, G.; Kathy, A. G.; Caldwell, K. D.; Giddings, J. C. *Int. J. Environ. Anal. Chem.* **1982**, *12*, 1–15.
- (34) Blo, G.; Contado, C.; Fagioli, F.; Rodriguez, M. H. B.; Dondi, F. *Chromatographia* **1995**, *41*, 715–721.
- (35) Thielking, H.; Kulicke, W. M. *Anal. Chem.* **1996**, *68*, 1169–1173.
- (36) Caldwell, K. D.; Cheng, Z. Q.; Hradecky, P.; Giddings, J. C. *Cell Biophys.* **1984**, *6*, 233–251.
- (37) Giddings, J. C.; Moon, M. H. *Anal. Chem.* **1991**, *63*, 2869–2877.
- (38) Moon, M. H.; Giddings, J. C. *Anal. Chem.* **1992**, *64*, 3029–3037.

and then passed through a 270-mesh sieve (having pores of  $\sim 53 \mu\text{m}$ ) to remove particles larger than  $\sim 50 \mu\text{m}$ . The particles were dried and then fractionated into six density classes for Sd/StFFF analysis (see later for the density classification). The total mass of particles passed through the sieve and those that did not pass were 51.6% and 3.6% of the original mass respectively, indicating that 44.8% of the original mass was from the soluble species. The fly ash suspensions for FFF analysis were prepared by dispersing the fly ash particles in an aqueous medium at a particle concentration of  $\sim 0.3\text{--}0.5\%$  (w/v). The suspensions were sonicated for 1 min prior to injection into FFF.

Various dispersing agents (surfactants) were tested for the preparation of fly ash suspensions. They include nonionic surfactants (Triton X-100, Tween 20, Tween 80, Tergitor NP-10, Nonidet P-40, poly(vinyl alcohol)), anionic surfactants (FL-70, sodium dodecyl sulfate, Aerosol 22, Triton X-200, Niaproof), and a cationic surfactant (cetyltrimethylammonium bromide (CTAB)). Detailed information on those surfactants is given in ref 39. All dispersing agents were purchased from Sigma Chemical Co. (St. Louis, MO) except FL-70, which was obtained from Fisher Scientific Co. (Pittsburgh, PA).

**Density Measurement for Fly Ash.** The bulk density of fly ash particles ( $\rho_{\text{ash}}$ ) is measured using a specific gravity bottle by

$$\rho_{\text{ash}} = \frac{C(D - A)}{V(C + D - B)} = \rho_w = \left( \frac{C}{C + D - B} \right) \quad (1)$$

where  $A$ ,  $B$ ,  $C$ , and  $D$  are the masses of the specific gravity bottle, the bottle containing water and fly ash, the fly ash sample, and the bottle filled with water, respectively.  $V$  is the volume of the specific gravity bottle, and  $\rho_w$  is the density of water. All measurements were made at room temperature. The measurement was repeated three times, and an average of the results was taken. The bulk density of fly ash was measured to be 2.43 g/mL with the relative error less than 7%.

**Sedimentation Field-Flow Fractionation (SdFFF).** The SdFFF system is similar to a model S100 available from FFFractionation, LLC (Salt Lake City, Utah). The SdFFF channel is 89.1 cm long (tip to tip), 1.1 cm in breadth, and 0.0127 cm in thickness. The rotor radius is 15.1 cm. The channel volume, measured by the elution volume of acetone, is 1.23 mL. The carrier solution was pumped by an Eldex metering CC-100-S-4 pump (Eldex Laboratories, Inc., Napa, CA). The eluted particles were monitored by a M720 UV/vis detector (Young-In Scientific Co., Seoul, Korea) operating at the fixed wavelength of 254 nm. The detector signal was processed using FFF software obtained from FFFractionation, LLC. Samples were injected using a model 7125 loop injector (Rheodyne, Inc., Cotati, CA). The injection volume was between 10 and 20  $\mu\text{L}$ , depending on the sample concentration.

**Fly Ash Suspension Stability Test.** To test the stability of fly ash suspensions prepared in various aqueous media, a Shimadzu model UV-1601 UV/vis spectrophotometer (Kyoto, Japan) was used. Transmittance was measured continuously for 10 min at the fixed wavelength of 254 nm.

**Optical and Electron Microscopy.** A Samwon CSB-HP3 model optical microscope (Samwon Scientific, Co., Seoul, Korea)

and a JEOL model JSEM-5410LV scanning electron microscope (JEOL, Tokyo, Japan) were used to determine the shape and size of the fly ash particles and to compare the sizes determined from Sd/StFFF and from a Coulter Multisizer.

**Carbon Analysis and Coulter Multisizer.** For determination of the carbon content of fly ash particles, an IDC Analyzer system multi N/C 3000 (AnalytikjenaAG, DE) was used. A Coulter Multisizer II (Beckman Coulter Inc., Fullerton, CA) was used to determine the sizes of the fly ash particles and to compare those sizes with the sizes obtained by Sd/StFFF. For Coulter counting measurements,  $\sim 2\text{--}3$  mg of fly ash was dispersed in 100 mL of the electrolyte Isoton II (a filtered, phosphate-buffered saline solution, PBS). The instrument was calibrated using monodisperse latex microspheres, supplied by Coulter, and Isoton II. The orifice size was 100  $\mu\text{m}$ , thus providing a dynamic range from  $\sim 2$  to 60  $\mu\text{m}$  of size.

## RESULTS AND DISCUSSION

**Size-Based Separation by Sd/StFFF.** In a simplified theory of Sd/StFFF, the retention time,  $t_r$  is inversely related to the diameter,  $d$ , by<sup>40</sup>

$$t_r = \frac{w^\theta}{3\gamma d} \quad (2)$$

where  $w$  is the channel thickness,  $\theta$  is the channel void time, and  $\gamma$  is a dimensionless "steric correction factor." The channel thickness ( $w$ ) and the channel void volume ( $\theta$ ) are constants. If the dimensionless factor,  $\gamma$ , is assumed to be a constant, it can be seen from eq 2 that  $\log t_r$  is linearly related with  $\log d$ . Thus, Sd/StFFF can provide size-based separations, where larger particles elute earlier than smaller particles.

Figure 1A shows a size-based Sd/StFFF separation of 10 polystyrene latex beads obtained under conditions usually used for Sd/StFFF separation of particulate samples. The carrier liquid was an aqueous solution of 0.1% FL-70 (added for the dispersion of particles) and 0.02% sodium azide (bactericide). The channel rotation rate was 1850 rpm and the flow rate was 6.5 mL/min. Figure 1A shows an excellent separation of particles in the  $\sim 2\text{--}40\text{-}\mu\text{m}$ -diameter range.

The dimensionless factor,  $\gamma$ , is not yet fully understood, mainly because of the presence of the hydrodynamic lift forces,<sup>41–45</sup> and thus, the size analysis in Sd/StFFF requires a calibration. Figure 1B shows the calibration curve ( $\log t_r$  vs  $\log d$ ) obtained from the retention data of each standard shown in Figure 1A. The curve, as expected, shows a good linearity, with a correlation coefficient of 0.999. The slope of the calibration curve ( $d \log t_r / d \log d$ ), which is defined as the size-based selectivity,  $S_d$ , was determined to be

(40) Giddings, J. C. *Chem. Eng. News*, **1988**, 66, 34–45.

(41) Peterson, R. E., II; Myers, M. N.; Giddings, J. C. *Sep. Sci. Technol.* **1984**, 19, 307–319.

(42) Williams, P. S.; Koch, T.; Giddings, J. C. *Chem. Eng. Commun.* **1992**, 111, 121–147.

(43) Williams, P. S.; Lee, S.; Giddings, J. C. *Chem. Eng. Commun.* **1994**, 130, 143–166.

(44) Williams, P. S.; Moon, M. H.; Xu, Y.; Giddings, J. C. *Chem. Eng. Sci.* **1996**, 51, 4477.

(45) Moon, M. H.; Lee, S. *J. Microcolumn Sep.* **1997**, 9, 565–570.

(39) Kim, W. S. Ph.D. Thesis, Yonsei University, Korea, 2001.

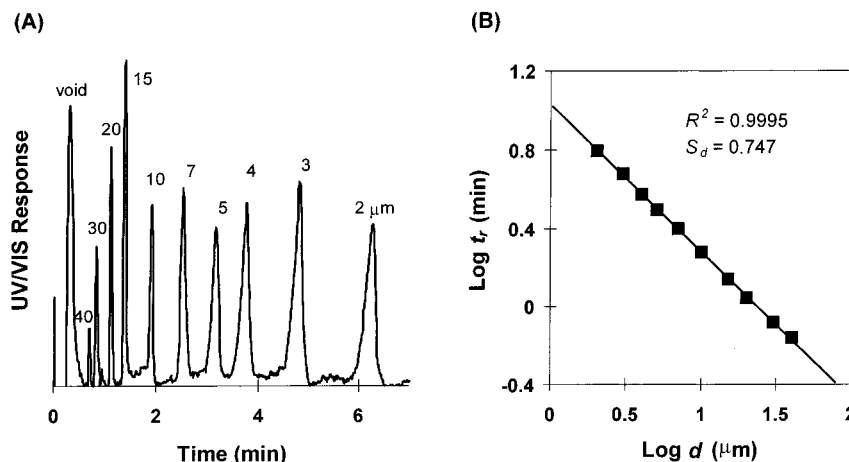


Figure 1. Sd/StFFF separation of polystyrene latex spheres (A) and a calibration plot (B). Experimental conditions are channel rotation rate, 1850 rpm; stop-flow time, 0.6 min; flow rate, 6.5 mL/min; and carrier liquid, water with 0.1% FL-70 and 0.02% NaN<sub>3</sub>.

0.747. Generally, the Sd/StFFF calibration curve is expressed by<sup>46</sup>

$$\log t_r = -S_d \log d + \log A \quad (3)$$

where  $A$  is a constant equal to the extrapolated value of the retention time  $t_r$  for the particles of unit diameter. The calibration curve shown in Figure 1B can be used to correlate the retention time and the particle size in Sd/StFFF. Assuming the band broadening is negligible, an Sd/StFFF fractogram can then be transformed into a size distribution by<sup>46</sup>

$$m(d) = c(t_r) \dot{V} S_d A \left( \frac{t_r}{A} \right)^{(S_d+1)/S_d} \quad (4)$$

where  $m(d)$  is the mass-based size distribution,  $c(t_r)$  is the fractogram signal, and  $\dot{V}$  is the flow rate through the channel. It is noted that the size distribution obtained from eq 4 may not be accurate for samples having narrow size distributions as a result of the band broadening.

In Sd/StFFF, retention depends on the density as well as the size.<sup>25</sup> Thus, for pure size-based separation, both the calibration standards and the sample need to have the uniform density, and also, the calibration standards must have the same density as that of the sample. If the density of the calibration standard is different from that of the sample, the density of the sample needs to be known. Then a density compensation<sup>46</sup> can be used in which the field strength (channel rotation rate) is adjusted for the sample to compensate the density difference between the standards and the sample. The adjusted channel rotation rate for the sample,  $(\text{rpm})_{\text{sample}}$ , can be calculated by<sup>45</sup>

$$(\text{rpm})_{\text{sample}} = \sqrt{\frac{\Delta\rho_{\text{std}}}{\Delta\rho_{\text{sample}}}} (\text{rpm})_{\text{std}} \quad (5)$$

where  $(\text{rpm})_{\text{std}}$  is the rotation rate for the standard runs,  $\Delta\rho_{\text{std}}$  is the density difference between the standard and the carrier, and  $\Delta\rho_{\text{sample}}$  is the density difference between the sample and the

Table 1. Compositions of Liquids Used for Density Classification of Fly Ash

| composition (vol %)  | density (g/mL) |
|--|----------------|
| CCl <sub>4</sub> 54% + CH <sub>2</sub> Br <sub>2</sub> 46%               | 2.0            |
| CCl <sub>4</sub> 9% + CH <sub>2</sub> Br <sub>2</sub> 91%                | 2.4            |
| CH <sub>2</sub> I <sub>2</sub> 15% + CH <sub>2</sub> Br <sub>2</sub> 85% | 2.6            |
| CH <sub>2</sub> I <sub>2</sub> 39% + CH <sub>2</sub> Br <sub>2</sub> 61% | 2.8            |
| CH <sub>2</sub> I <sub>2</sub> 63% + CH <sub>2</sub> Br <sub>2</sub> 37% | 3.0            |

carrier. With the density compensation, the particles having the same size are subjected to the same centrifugal force irrespective of density, and thus, they elute at the same time. With the density compensation, a calibration based on standards having a different density from that of the sample can be used for size determination of the sample.

**Density-Classification of Fly Ash.** The size characterization by Sd/StFFF is complicated if the sample has a broad density distribution, even with the density-compensation. Particles may elute together, even if they have different sizes, so long as they have the same combination of size and density that yields the same retention. It has been reported that fly ash contains particles of various chemical compositions, including char and silica-rich particles in less dense classes, and iron-, calcia- and alumina-rich particles in denser classes.<sup>7</sup> To remove the influence of the density variation, the original fly ash was fractionated into a few different density classes prior to Sd/StFFF analysis.

A standard centrifugal procedure<sup>14</sup> was employed for density classification of the fly ash. For density classification, liquids having densities of 2.0, 2.4, 2.6, 2.8 and 3.0 g/mL were prepared by mixing carbon tetrachloride, dibromomethane, and diiodomethane (whose densities were 1.594, 2.477 and 3.31 g/mL respectively) in various proportions as shown in Table 1. All densities were at 25 °C. First, a dilute fly ash suspension was prepared in *n*-butanol at a concentration of ~0.01 g/mL. The suspension was then sonicated in a probe-type sonicator to break aggregated particles, if any, for 1.5 min under moderate power (30 W). Disaggregation is necessary, because the presence of aggregated particles, particularly those formed by aggregation of particles having different densities, causes the density classification to be inaccurate. The *n*-butanol was chosen as a suspension liquid,

(46) Giddings, J. C.; Moon, M. H.; Williams, P. S.; Myers, M. N. *Anal. Chem.* **1991**, *63*, 1366–1372.



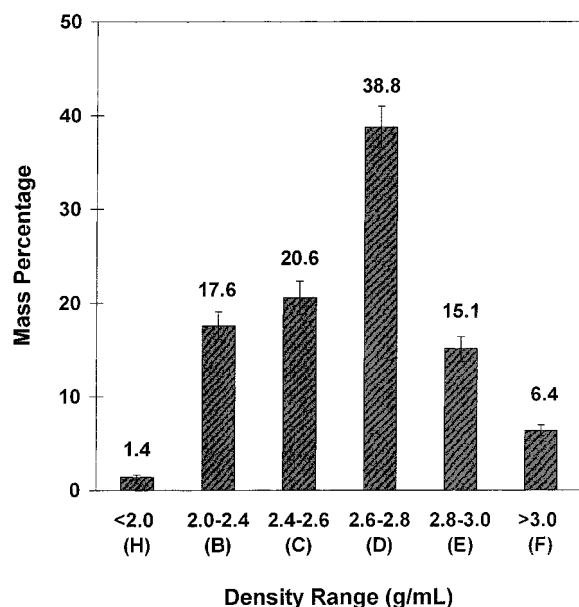


Figure 2. Mass percentage of six density fractions of fly ash.

because it wets the fly ash particles well with minimum leaching. After the sonication, the suspension was centrifuged for 10 min to separate the ash particles into two subpopulations (particles having higher or lower density than that of the liquid). During centrifugation, the centrifuge speed was gradually increased to up to 3000 rpm, at which point the particles were subjected to an acceleration of about 1000 G.

The centrifugal separation was first performed with the liquid having the density of 2.6 g/cm<sup>3</sup> and then with the liquids having a density of 2.4 and 2.8 for the floats and the sinks, respectively, and so on. A total of six density fractions of fly ash particles were obtained (labeled fraction H and B–F). The density classification was repeated three times, and the averaged results are shown in Figure 2. It can be noted that the total mass of the six density fractions was 73.5% of the original mass, indicating 26.5% of mass was leached out during the density classification. The leached-out fraction was also collected (labeled fraction G). The mass percentage of each fraction shown in Figure 2 is the percentage of the total mass of the six fractions (not of the original mass). As expected, fly ash has a broad density distribution, with ~40% of particles having densities between 2.6 and 2.8 g/mL (fraction D).

Figure 3 shows pictures of vials containing fly ash particles. From the left, the first is the original fly ash sample (labeled A), followed by the leached-out fraction (labeled G), then the six density fractions (labeled H and B–F) in increasing order of density. The less dense particles are blackish, and as the density increases, the particles become colored, indicating more of the inorganic metal oxides (such as calcium oxide (lime), alumina, and ferric oxide) are present. The particles in the leached-out fraction G and the less-dense fraction H (having a density lower than 2.0) are much darker, probably because of the presence of carbonaceous particles having lower densities. This observation is confirmed by the total carbon analysis shown in Figure 4, where the total carbon content (organic + inorganic carbon content) decreases as the density increases.

**Selection of Dispersing Agent.** Fly ash collected in particulate cleanup devices (such as the bag filter used in this study) may contain highly agglomerated particles, and, thus, cannot be sized directly in a dry state. Proper dispersing agents and dispersing methods need to be selected to minimize the particle–particle and the particle–wall interactions to reduce the aggregation of particles. A good dispersing agent surrounds the particles in a monolayer and minimizes the particle–particle interaction.<sup>47</sup>

For the selection of a dispersing agent, the suspension stability was tested by the continuous monitoring for 10 min of the transmittance (*T*) of the fly ash suspensions prepared in various media using an UV/vis spectrophotometer. Fly ash suspensions were prepared by dispersing the original fly ash using a probe-type sonicator for 2 min at concentrations of 0.1% (w/v). Fourteen different combinations of concentration and types of the dispersing agent were tested, and 11 of them are shown in Figure 5. Generally, transmittance increases with time as the particles settle. It seems 0.1% FL-70 provides the best performance as a dispersing agent. The transmittance of the fly ash suspension prepared in 0.1% FL-70 was very close to zero (providing a strong signal when UV/vis absorbance detector was used for Sd/StFFF, as in this study) and stayed almost the same during the whole measurement period of 10 min (providing high suspension stability). The fly ash suspension in 0.5% FL-70 showed a very similar trend. Unfortunately, the Sd/StFFF data of fly ash suspensions prepared in 0.1 or 0.5% FL-70 showed poor reproducibility.

The 50% ethanol, 0.05% CTAB, and 0.1% Tween 80 also showed good performances as dispersing agents. The transmittance data were very similar to each other (only the data for 50% ethanol is shown in Figure 5). Among the various dispersing agents tested, the 50% ethanol was finally chosen, because it is easier to handle and yielded the most consistent Sd/StFFF data.

**Selection of Sd/StFFF Carrier Liquid.** The choice of FFF carrier is also important. In previous experiences with other environmental particles, water alone could cause irreversible particle-aggregation. The addition of surfactant proved to be helpful in reducing particle–particle and particle–wall interactions, thus reducing particle aggregation and sample loss. The use of alcohol in SdFFF was somewhat limited, because it can swell the sealant and glue in the SdFFF channel. Water with various concentrations of FL-70 was tested as a carrier liquid for the SdFFF analysis of fly ash dispersed in 50% ethanol. An aqueous solution of 1.0 % FL-70 was finally chosen, because it yielded Sd/StFFF fractograms with minimum distortions in the fractogram (such as fronting or tailing, etc). The fly ash did not elute well at concentrations of FL-70 lower than 1.0%.

**Sd/StFFF of Fly Ash.** As mentioned earlier, the size analysis by Sd/StFFF requires a calibration. Figure 6A shows an Sd/StFFF fractogram of the same polystyrene mixture shown in Figure 1 obtained with 1.0% FL-70 as the carrier. The fractogram shows a good separation again and yields a linear calibration curve (Figure 6B). The calibration curve shown in Figure 6B cannot be used directly for size determination of fly ash, because the density of fly ash is different from that of the polystyrene standard. The bulk density of the fly ash was measured to be 2.43 g/mL and was higher than that of the polystyrene beads (1.05 g/mL). The density

(47) Conley, R. F. *Practical Dispersion: A Guide to Understanding and Formulating Slurries*; VCH: New York, 1996.

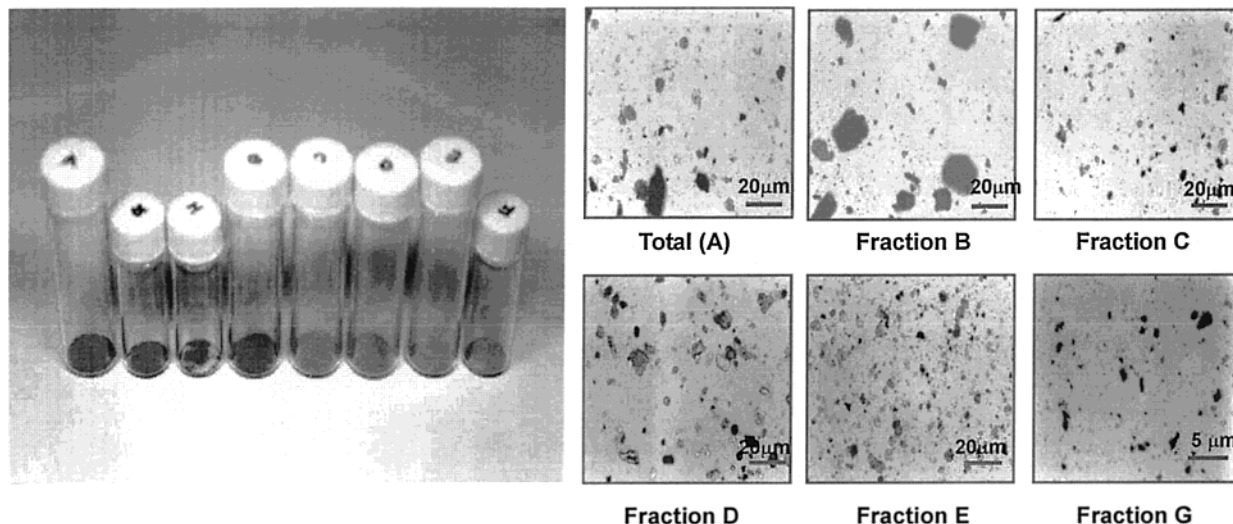


Figure 3. Pictures and micrographs of original and density fractions of fly ash.

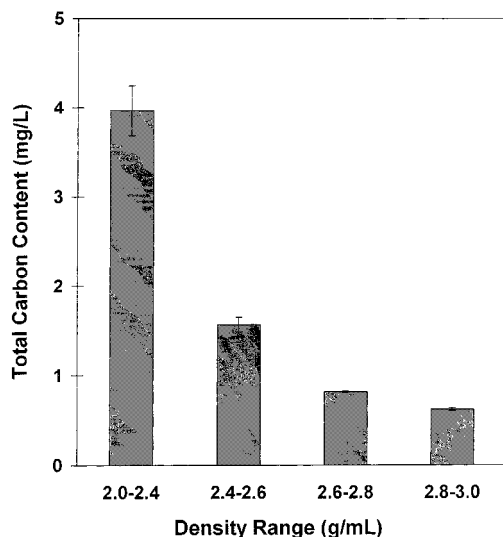


Figure 4. Total carbon content of density fractions of fly ash.

compensation was thus needed, and the adjusted channel-rotation rate for the Sd/StFFF analysis of the fly ash was calculated by eq 5 to be 346 rpm.

Figure 7 shows an Sd/StFFF fractogram of the original fly ash obtained at the field strength of 350 rpm and at the flow rate of 6.12 mL/min. The sample suspension was prepared by dispersing the fly ash particles in an aqueous solution of 50% ethanol. The carrier liquid was an aqueous solution of 1.0% FL-70. The optical micrographs of the 4 slices taken from the fractogram confirm the size-based Sd/StFFF separation, where the particle size decreases as the retention time increases. It can be seen that the fly ash particles are of irregular shapes.

Figure 8 shows Sd/StFFF fractograms of the four density fractions (fractions B–E). All of the preparation and experimental conditions were the same as those in Figure 7 except the field strength, which was adjusted for each fraction for density compensation. The field strength for the density compensation was calculated for each fraction using eq 4 and is summarized in Table 2. It seems no particular relationship exists between the density and the size distribution.

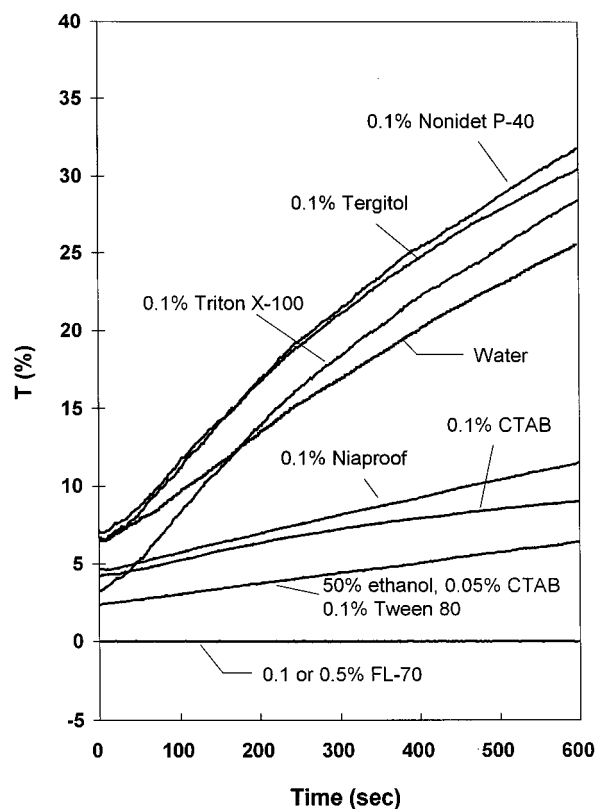


Figure 5. UV-vis transmittance of fly ash suspensions prepared in various suspension media. The fly ash suspensions are prepared by dispersing the original fly ash in various media at a concentration of 0.1% (w/v) by probe-type sonication for 2 min.

The fractograms shown in Figure 8 can be converted to size distributions using eq 4. Figure 9 shows the size distributions of fraction D obtained by Sd/StFFF (filled circles) and by the Coulter Multisizer (open squares). The size distribution from Sd/StFFF shows the sample has a broad size distribution, as normally expected for fly ash. The Coulter Multisizer yields a number distribution in which the number of particles in each size interval is counted independently. The size distribution from Sd/StFFF

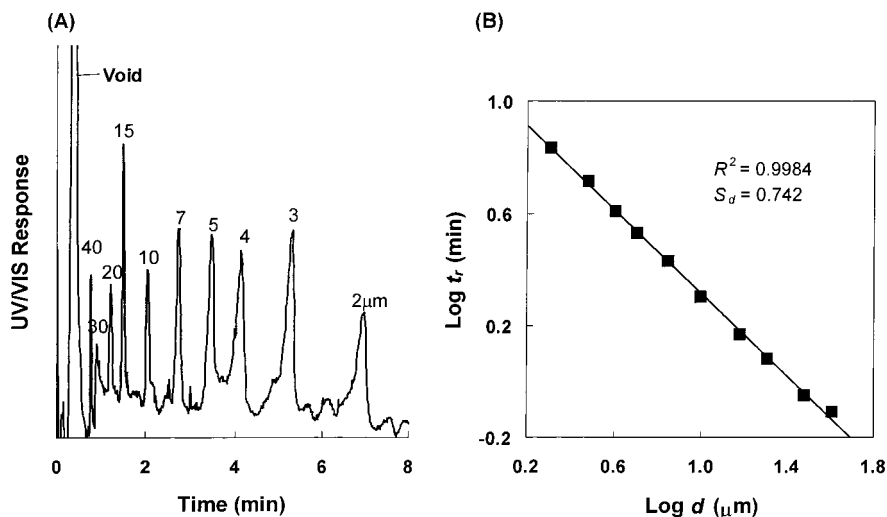


Figure 6. Sd/StFFF separation of polystyrene latex spheres (A) and a calibration plot (B). The sample mixture and the experimental conditions are the same as those in Figure 1, except that the flow rate is 6.12 mL/min, and the carrier liquid is water with 1.0% FL-70.

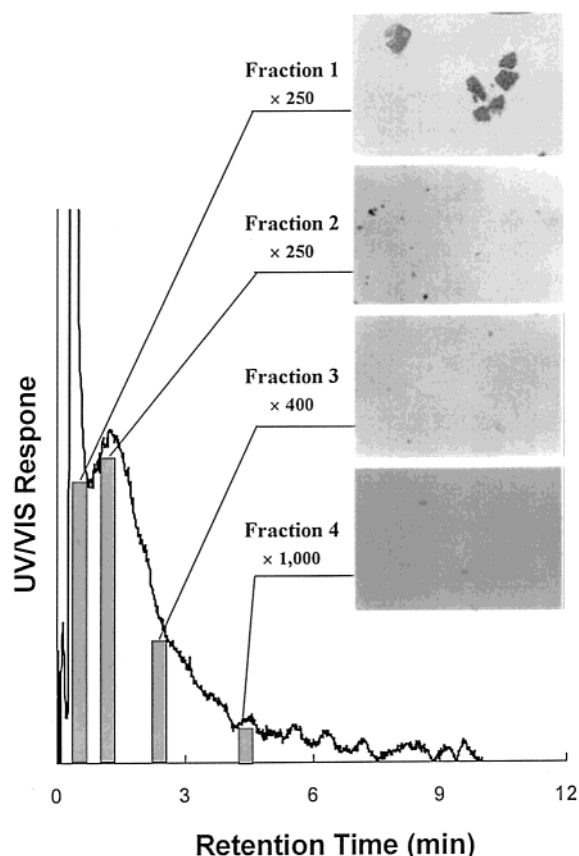


Figure 7. Sd/StFFF fractogram of the original fly ash obtained at the same conditions as in Figure 6, except that the field strength is now lowered to 350 rpm for density compensation.

is converted to the number distribution (represented by crosses in Figure 9) by recalculating  $m(d)$  with  $c(t_r)$  obtained by dividing the fractogram signal by  $d^{4.46}$ . The number distribution from Sd/StFFF then shows better agreement with the distribution from the Coulter Multisizer. There still exists some degree of discrepancy: the distribution from the Coulter Multisizer is shifted left (toward smaller sizes) with respect to that from Sd/StFFF. This may be attributed to the irregularity in the shapes of the fly ash particles. Previous studies showed that in Sd/StFFF, the non-

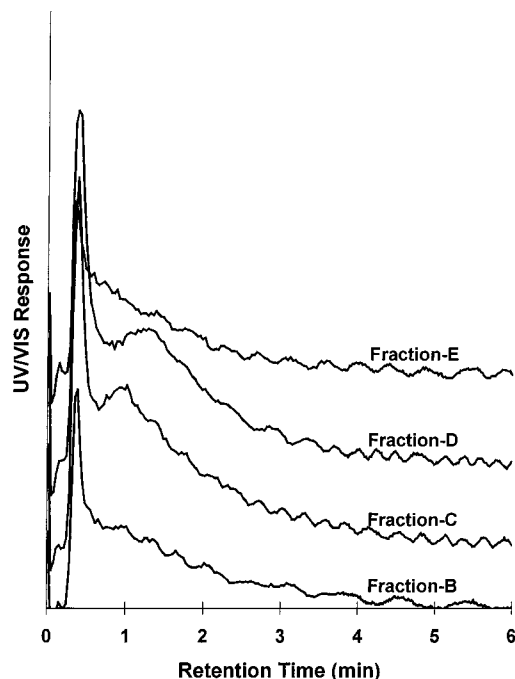


Figure 8. Sd/StFFF fractograms of the density fractions B–E. Experimental conditions are the same as those in Figure 6, except the field strengths. Field strength is adjusted for density compensation of each fraction.

spherical particles tend to elute earlier than spheres of the same volume as a result of greater lift forces acting on them, resulting in the measured diameter of nonspherical particles larger than the diameter of spheres of the same volume.<sup>48,49</sup> Similar trends were observed for other density fractions between data obtained from Sd/StFFF and the Coulter Multisizer. The sizes obtained from Sd/StFFF were also larger than those from micrographs.

## CONCLUSIONS

A Sd/StFFF method was developed for the separation and the size characterization of fly ash emitted from municipal waste

(48) Beckett, R.; Jiang, Y.; Liu, G.; Moon, M. H.; Giddings, J. C. *Part. Sci. Technol.* **1994**, *12*, 89–113.

(49) Beckett, R.; Giddings, J. C. *J. Colloid Interface Sci.* **1997**, *186*, 53–59.

Table 2. Density-Compensated Field Strengths for Fly Ash Samples

| sample     | density range (g/mL) | av density $\rho_{av}$ , (g/mL) | $\Delta\rho$ ( $\rho_{\text{sample}} - \rho_{\text{solvent}}$ ) (g/mL) | RPM for density compensation |
|------------|----------------------|---------------------------------|--|------------------------------|
| original   |                      | 2.43                            | 1.43   | 346                          |
| fraction B | 2.0–2.4              | 2.2                             | 1.2  | 378                          |
| fraction C | 2.4–2.6              | 2.5                             | 1.5  | 338                          |
| fraction D | 2.6–2.8              | 2.7                             | 1.7  | 317                          |
| fraction E | 2.8–3.0              | 2.9                             | 1.9  | 300                          |
| fraction F | >3.0                 |                                 |  |                              |

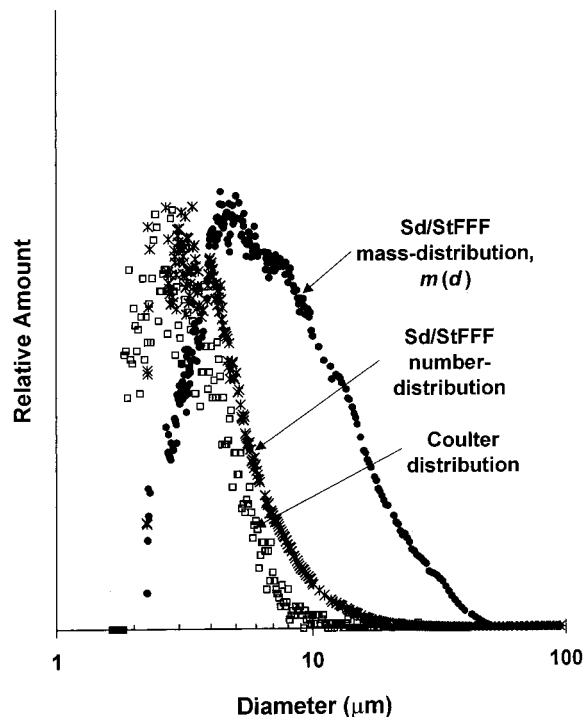


Figure 9. Size distributions of density fraction D (density range ~2.6–2.8) obtained by Coulter Multisizer and Sd/StFFF.

incinerators. Various experimental parameters were tested for the optimization of Sd/StFFF and are summarized in Table 3. As in most other sizing techniques, the sizes are determined in Sd/StFFF by using a calibration curve (usually made with spherical standards), and thus, they are not absolute. Still, Sd/StFFF usually yields fairly accurate sizes for spherical or near-spherical particles. The fly ash size distributions determined by Sd/StFFF tend to shift toward larger sizes with respect to those obtained from the Coulter Multisizer or microscopy, probably as a result of the

Table 3. Sd/StFFF Conditions for Size Analysis of Incinerator Fly Ash

|                   |   |
|-------------------|---|
| suspension concn  | $\approx 0.3\%$ (w/v)                   |
| dispersing agent  | doubly distilled water with 50% ethanol |
| dispersing method | tip sonication (1.5 min), vortexing     |
| carrier liquid    | doubly distilled water with 1.0% FL-70  |
| ionic strength    | $\approx 0.012$ M                       |

irregular shapes of the fly ash particles; however, the results suggest Sd/StFFF has the potential to be a useful tool for the characterization of fly ash particles. It actually provides separation (and, thus, elution) of fly ash particles based on size and allows the collection of narrow fractions, which can be subjected to further analysis. Currently, work is underway for the analysis of fly ash using FFF and related techniques. This includes the combination of Sd/StFFF with SPLITT fractionation (SF) and the composition analysis of density fractions, among others.

#### ACKNOWLEDGMENT

This study was supported by Grant no. 1999-124-001-5 from the interdisciplinary research program of the KOSEF. The authors thank Dr. Myeong Hee Moon of the Department of Chemistry, Pusan National University, and Dr. Yoon-Seok Chang of the School of Environmental Engineering, Pohang University of Science & Technology, for providing of the fly ash samples.

Received for review August 21, 2001. Accepted November 5, 2001.

AC010937Y